

## Chapter 9

### Conclusions and The Future

In this chapter I will specify some conclusions that can be drawn by combining the results presented in this thesis with earlier studies of cometary nuclei. Of course my work has not made the sample of nuclei complete, and a few dozen more objects with well-determined physical properties would be helpful before any analysis becomes statistically defensible. However it is interesting to collate the current information and see what trends may be appearing, and what observational biases are dominating the study of comets.

#### 9.1 Comets and Their Disguised Relations

Figure 9.1 shows a plot of the effective diameters and geometric albedos for several cometary nuclei, including the ones I have discussed in this thesis. Also plotted are nuclei studied by others, and several NEAs and Centaurs. The data are listed in Table 9.1, with the information from this thesis having an arrow in the “Ref.” column. Not all data in Table 9.1 are plotted on Fig. 9.1. Here are some caveats about this table:

- Most of the entries are from reports of a nuclear size measurement made using thermal infrared techniques. In a few cases, radar or optical observations that have spatially-resolved images of the object were used. Observations in those wavelength regimes that just have cross section-integrated photometry were not used.

- The vast majority of the radii and albedos were derived using the Standard Thermal Model. A few used the Rapid Rotator Model, and one was even derived from the Isothermal Model. I have not made an attempt to reanalyze these data, I simply have quoted the values and errors that the authors themselves state, even though there are very clearly cases where the error bars are underestimated. Considering the uncertainties in some of the parameters that go into the thermal models (such as the beaming factor and the phase behavior; Chapter 3), the systematic error of the absolute flux calibration (about 5%, Tokunaga 1984, Rieke *et al.* 1985), and the experience of the several comets presented in this thesis, it seems that some of the diameters’ error bars could be closer to 20%, and the albedos’ error bars closer to 40%. This is especially true where the thermal data is of low  $S/N$ , and this does not even include any systematic error with using an idealized model. Exceptions to this include but are not limited to: Comet Halley and Asteroid (433) Eros, which have been optically imaged with sub-km spatial resolution; Asteroid (4179) Toutatis, which has been the subject of multiple extensive radar experiments; and Comet *IRAS-Araki-Alcock*, which passed so close to Earth and resulted in a multiwavelength data cache so large that it was probably only a matter of time before someone collated everything into a coherent picture (Sekanina 1988c).

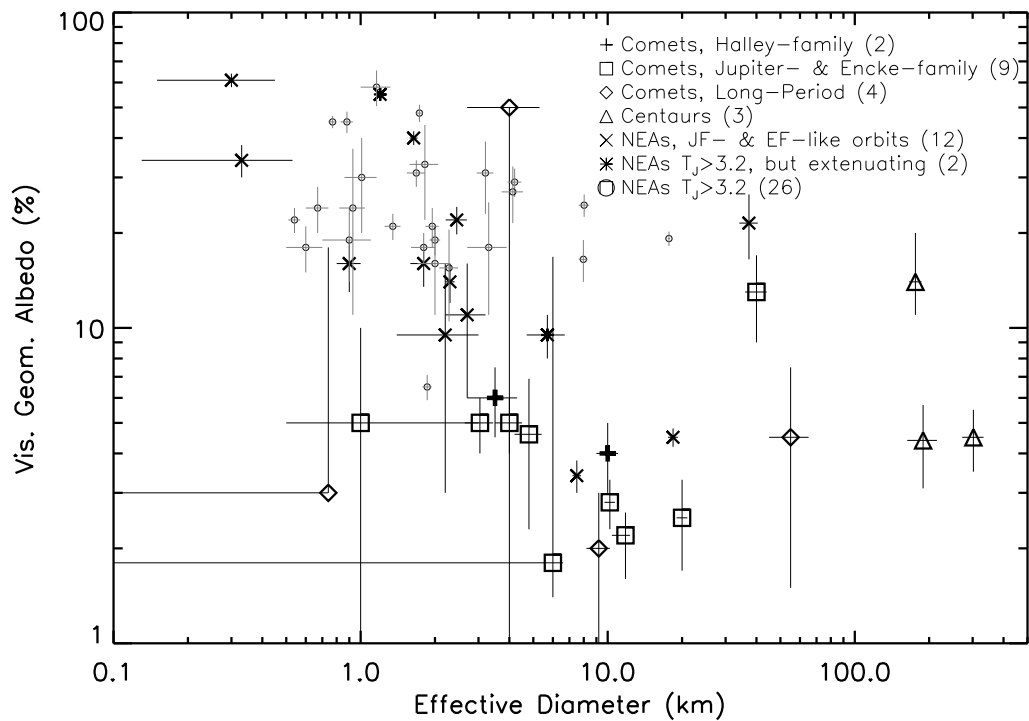


Figure 9.1: The sizes and albedos of active cometary nuclei, some near-Earth asteroids, and Centaurs. The “cometary” region is now starting to fill out, thanks to many thermal studies done since the mid-1990s.

- One notices that some cometary diameters have no attendant albedos. Ironically it is often the case that reliable optical cross sections do not exist for the comets that have been observed in the mid-IR. In the future, more coordination between observations in the multiple wavelength regimes is needed. In Chapter 1 I discussed some of the problems of nucleus observation that contribute to this lack of optical cross sections.

- The “Rotation?” column shows many more entries with “N” than with “Y,” i.e. for most of the listed objects, the rotational context is unknown. This has not been reflected in the error bars of the diameters and albedos, so the true error bars are even higher for many objects. For some objects this is not a problem because the observations took so long that the rotational variation has probably been averaged out, and so is incorporated into the error estimate already. For example, the multiple mid-IR exposures of Hyakutake cover several hours of time, and hence a large fraction of the rotation period.

- Note that the “Cometary Nuclei” in the title is in quotation marks. I have included many asteroids in the table, some fraction of which are extinct comets. I will now discuss this point in more detail.

The Tisserand parameter,  $T_J$ , is a constant of motion in a restricted three-body problem. Considering the Sun, Jupiter, and a small body as the three members of a system, as long as the body is not having a close encounter with Jupiter at the time of the observation, the value of  $T_J$  is constant. In practice the value fluctuates by a few percent due to perturbations by other planets. The definition is (Danby 1962, p.189):

$$T_J = \frac{a_J}{a} + 2 \cos i \sqrt{\frac{1 - e^2}{a_J/a}}, \quad (9.1)$$

where  $a_J$  is the semimajor axis of Jupiter, 5.2 AU,  $a$  is the object’s semimajor axis,  $e$  is the object’s eccentricity, and  $i$  is the object’s orbital inclination. Tisserand himself recognized in the late 19th century that this constant of motion could be used to identify two comets observed far apart in time as the same object, if the comet had had a close encounter with Jupiter in the interval and thus had its orbital elements drastically changed.

The value of the parameter indicates the strength of the dynamical coupling of the object’s orbit to Jupiter. Most asteroids have  $T_J > 3$ , while the short-period comets mostly have  $T_J < 3$ ; i.e.,  $T_J = 3$  is the boundary between the coupling – almost all short-period comets are dynamically coupled to Jupiter, while most asteroids are not. An indication of this can be seen in the  $q_{ap}$  column in Table 9.1; for objects with  $2 < T_J < 3$ , the aphelion is close to Jupiter.

Of course the  $T_J = 3$  border is not perfect. There are asteroids that have  $T_J < 3$  – these are usually NEAs with a sufficiently large aphelion distance – and there are comets that have  $T_J > 3$  – the so-called “Encke” Family (Levison 1996), which so far only has two known members, both of which are in Table 9.1. These are comets in more classic NEA orbits, i.e. the aphelion distance is never high enough to bring them close to Jupiter.

The explanation for the asteroids in cometary orbits follows from the supposed typical life cycle of a short-period Jupiter Family comet. After being perturbed

out of the Kuiper Belt and into the outer planetary region, the nucleus is at the mercy of the gas giants. Approximately thirty percent of these comets that leave the Kuiper Belt become part of the Jupiter Family (Levison and Duncan 1997); the rest are either ejected or sent farther out in the Solar System. Centaurs are thought to be Kuiper Belt objects currently in transition, since their dynamical lifetimes is roughly only  $10^6$  year (Dones *et al.* 1996).

Once an object is in the Jupiter Family, its dynamical lifetime there is about  $10^5$  years (Wetherill 1991), after which the comet collides with a planet or the Sun, or is sent into a classic NEA orbit, decoupled from Jupiter. Of course during those  $10^5$  years the comet is outgassing, since it passes close enough to the Sun, but the store of volatile material in the comet will only last about  $10^4$  years – either the comet will disintegrate by then or the mantled surface will be too thick, choking off the available ice (Levison and Duncan 1997). Hence on average a comet will become dormant while still coupled to Jupiter. Observationally, one would discover an asteroid in a comet-like orbit ( $T_J < 3$ ), a few of which are noted in Table 9.1. However it is possible that a comet will be quickly sent into an NEA orbit and decoupled from Jupiter before all available ice is gone, and we will see active comets in NEA ( $T_J > 3$ ) orbits, which we do see most famously as comet Encke. The existence of this comet and comet Wilson-Harrington guarantee that, despite the fact that the Main Belt can potentially provide a large fraction of the kilometer-size and larger NEAs (Rabinowitz 1997), some fraction of the NEAs must be dead cometary nuclei. The trick, which we have not yet solved, is to find some diagnostic that indicates which of the NEAs are cometary and which are asteroidal (McFadden 1994). Future studies of NEAs and nuclei may shed light on this problem.

In Table 9.1 I have made an arbitrary separation at  $T_J = 3.2$  to mark which asteroids might dynamically have a higher probability of being dead comets. However, there are two intriguing asteroids that have high  $T_J$  and yet could very well be cometary. Asteroid (3200) Phaethon is the parent to the Geminid meteor stream (Whipple 1983), which is strong evidence for a cometary origin, despite the fact that its aphelion distance is almost 2 full AU smaller than the next smallest cometary one (Encke). Asteroid (2201) Oljato was observed to have a transient blue excess by McFadden *et al.* (1993), which they argued was caused by a cometary outburst. One problem with Oljato is its high albedo, much higher than all of the known cometary nuclei. Nevertheless, I have separated these objects from the other high  $T_J$  crowd to emphasize that these objects have additional extenuating circumstances.

Immediately one notices that there are some very black asteroids in both the low- $T_J$  and high- $T_J$  sections. In my opinion these objects are the prime candidates for being extinct nuclei and further study is needed to find out if there is any distinguishing characteristic observable from Earth that separates them from the other, Main Belt-derived NEAs.

Furthermore, there are many asteroids, such as (944) Hidalgo, (5335) Damocles, and 1984 BC that have low  $T_J$  – 2.07, 1.15, and 2.78 respectively – but that simply have not yet had their thermal flux measured. Presumably, when that happens, they will take their place alongside the other low-albedo objects.

**Table 9.1: Sizes and Albedos of “Cometary Nuclei”**

Object	Diameter	Albedo	$T_J$	$q_{ap}$	Rotation?	Ref.	In Fig.
	(km)	(%)		(AU) <sup>a</sup>	<sup>b</sup>	<sup>c</sup>	9.4?
<i><u>Halley Family Comets</u></i>							
1P/Halley	$10 \pm 1$	$4 \pm 1$	-0.61	35.3	NA	2	Y
55P/Tempel-Tuttle	$3.5 \pm 0.8$	$6 \pm 1.5$	-0.64	19.7	N	<b>1</b> ←	Y
“	$3.3 \pm 0.3$	$4.5 \pm 1$	-0.64	19.7	N	3	N
109P/Swift-Tuttle	$15 \pm 3$	<sup>d</sup>	-0.28	51.7	N	35	N
126P/ <i>IRAS</i>	$< 2.86 \pm 0.16$	<sup>d</sup>	1.96	9.5	N	3	N
<i><u>“Encke” Family Comets</u></i>							
2P/Encke	$4.8 \pm 0.6$	$4.6 \pm 2.3$	3.03	4.1	Y	<b>1</b> ←	Y
107P/(4015) Wilson-Harrington	$4.0 \pm 0.5$	$5 \pm 1$	3.08	4.3	N	4	Y
<i><u>Jupiter Family Comets</u></i>							
6P/d’Arrest	$\sim 3.5$	<sup>d</sup>	2.71	5.6	N	34	N
10P/Tempel 2	$11.8^{+0.5}_{-1.4}$	$2.2^{+0.4}_{-0.6}$	2.96	4.7	Y	5	Y
21P/Giacobini-Zinner	$\sim 2$	$\sim 5$	2.47	6.0	N	31	Y

Table 9.1 – cont'd

Object	Diameter	Albedo	$T_J$	$q_{ap}$	Rotation?	Ref.	In Fig.
	(km)	(%)		(AU) <sup>a</sup>	<i>b</i>	<i>c</i>	9.4?
<i>Jupiter Family Comets (cont'd)</i>							
22P/Kopff	$3.04 \pm 0.4$	$5 \pm 1$	2.87	5.3	N	3	Y
24P/Schaumasse	$< 6.6$	<i>d</i>	2.51	6.9	N	36	N
28P/Neujmin 1	$20 \pm 1$	$2.5 \pm 0.8$	2.16	12.3	Y	6	Y
29P/Schwassmann-Wachmann 1	$40 \pm 4$	$13 \pm 4$	2.99	6.3	N	7	Y
49P/Arend-Rigaux	$10.2 \pm 0.5$	$2.8 \pm 0.5$	2.71	5.7	Y	8	Y
81P/Wild 2	$< 6.0 \pm 1.2$	$> 1.8 \pm 0.4$	2.88	5.3	N	<b>1</b> ←	Y
103P/Hartley 2	$< 1.16 \pm 0.24$	<i>d</i>	2.64	5.85	N	3	N
<i>Oort-sense Old Long-Period Comets</i>							
C/1983 H1 IRAS-Araki-Alcock	$9.2 \pm 1$	$2 \pm 1$	<i>e</i>	<i>e</i>	Y	32	Y
C/1983 J1 Sugano-Saigusa-Fujikawa	$\lesssim 0.74$	$\gtrsim 3$	<i>e</i>	<i>e</i>	N	33	N
C/1995 O1 Hale-Bopp	$50 \pm 10$	$4.5 \pm 3$	<i>e</i>	<i>e</i>	N	<b>1</b> ←	Y
C/1996 B2 Hyakutake	$4 \pm 1.3$	$< 50$	<i>e</i>	<i>e</i>	N	29,30, <b>9</b> ←	Y

Table 9.1 – cont'd

Object	Diameter	Albedo	$T_J$	$q_{ap}$	Rotation?	Ref.	In Fig.
	(km)	(%)		(AU) <sup>a</sup>	<i>b</i>	<i>c</i>	9.4?
<u>Oort-sense Old Long-Period Comets (cont'd)</u>							
C/1997 T1 Utsumomiya	$< 11.6 \pm 4.0$	<i>d</i>	<i>e</i>	<i>e</i>	N	<b>1</b> ←	N
C/1998 U5 LINEAR	$\sim 2$	<i>d</i>	<i>e</i>	<i>e</i>	N	31	N
<u>Oort-sense New Long-Period Comets</u>							
<b>None</b>							
<u>Centaur</u>							
95P/(2060) Chiron	$176 \pm 10.$	$14_{-3}^{+6}$	3.36	18.95	N	10	N
(5145) Pholus	$189 \pm 26.$	$4.4 \pm 1.3$	3.20	31.8	N	11	N
(10199) 1997 CU <sub>26</sub>	$302 \pm 30.$	$4.5 \pm 1.0$	3.48	18.4	N	12	N
<u>NEAs with Low <math>T_J</math></u>							
(1036) Ganymed	$37.3 \pm 3.2$	$21.5 \pm 5$	3.03	4.1	N	13	N
(1580) Betulia	$7.5 \pm 0.3$	$3.4 \pm 0.4$	3.07	3.3	N	14	Y
(1915) Quetzalcoatl	$0.33 \pm 0.2$	$34 \pm 4$	3.12	4.0	N	13	N

Table 9.1 – cont’d

Object	Diameter	Albedo	$T_J$	$q_{ap}$	Rotation?	Ref.	In Fig.
	(km)	(%)		(AU) <sup>a</sup>	<sup>b</sup>	<sup>c</sup>	9.4?
<u>NEAs with Low <math>T_J</math> (cont’d)</u>							
(2608) Seneca	$0.9 \pm 0.1$	$16 \pm 3$	3.17	3.95	N	15	Y
(3360) 1981 VA	$1.80 \pm 0.21$	$16 \pm 2.5$	2.97	4.3	N	13	Y
(4179) Toutatis	$2.8 \pm 0.1$	$17.5 \pm 1.5$	3.15	4.1	Y	16 <sup>f</sup>	Y
(4197) 1982 TA	$1.64 \pm 0.06$	$40 \pm 2.$	3.09	4.1	N	13	N
(3552) Don Quixote	$18.39 \pm 0.85$	$4.5 \pm 0.3$	2.31	7.3	N	13	Y
(6063) Jason	$1.4 \pm 0.1$	$16 \pm 2$	3.19	3.9	N	17	Y
(6178) 1986 DA	$2.3 \pm 0.1$	$14 \pm 2$	3.04	4.5	N	18	Y
(6489) Golevka	$0.30 \pm 0.01$	$61 \pm 3$	3.18	4.0	Y	19	N
1983 VA	$2.7 \pm 0.1$	$7 \pm 1$	2.97	4.4	N	20	Y
<u>NEAs with High <math>T_J</math> but Extenuating Circumstances</u>							
(2201) Oljato	$1.20 \pm 0.05$	$55 \pm 2$	3.30	3.7	N	13	N
(3200) Phaethon	$4.7 \pm 0.5$	$14 \pm 3$	4.51	2.4	N	21,22	Y



Table 9.1 – cont’d

Object	Diameter	Albedo	$T_J$	$q_{ap}$	Rotation?	Ref.	In Fig.
	(km)	(%)		(AU) <sup>a</sup>	<sup>b</sup>	<sup>c</sup>	9.4?
<u>NEAs with High <math>T_J</math></u>							
(433) Eros	$18 \pm 1$	$19 \pm 3$	4.58	1.8	NA	28 <sup>f</sup>	N
(887) Alinda	$4.13 \pm 0.41$	$27 \pm 5.5$	3.22	3.9	N	13	N
(1566) Icarus	$0.88 \pm 0.04$	$45 \pm 3.5$	5.30	2.0	N	13	N
(1620) Geographos	$1.95 \pm 0.12$	$21 \pm 3$	5.07	1.7	N	13	N
(1627) Ivar	$7.97 \pm 0.33$	$16.5 \pm 2.5$	3.88	2.6	N	13	N
(1685) Toro	$3.20 \pm 0.25$	$31 \pm 8$	4.72	2.0	N	13	N
(1862) Apollo	$1.35 \pm 0.1$	$21 \pm 2$	4.41	2.3	N	27	N
(1863) Antinous	$1.8 \pm ?$	$18 \pm ?$	3.30	3.6	N	18 <sup>g</sup>	N
(1865) Cerberus	$0.93 \pm 0.11$	$24 \pm 13$	5.59	1.6	N	13	N
(1866) Sisyphus	$8.03 \pm 0.4$	$24.5 \pm 2$	3.51	2.9	N	13	N
(1943) Anteros	$1.68 \pm 0.14$	$31 \pm 3$	4.64	1.8	N	13	N
(1980) Tezcatlipoca	$4.20 \pm 0.27$	$29 \pm 3$	4.00	2.3	N	13	N

Table 9.1 – cont’d

Object	Diameter	Albedo	$T_J$	$q_{ap}$	Rotation?	Ref.	In Fig.
	(km)	(%)		(AU) <sup>a</sup>	<sup>b</sup>	<sup>c</sup>	9.4?
<i>NEAs with High <math>T_J</math> (cont’d)</i>							
(2062) Aten	$0.9 \pm 0.2$	$19 \pm 5$	6.18	1.1	N	25,26	N
(2100) Ra-Shalom	$2.48 \pm 0.35$	$13 \pm 4$	6.94	1.2	N <sup>h</sup>	23	N
“	$2.04 \pm 0.1$	$11.5 \pm 1$	6.94	1.2	N	15	Y
“	$1.67 \pm 0.1$	$21 \pm 3$	6.94	1.2	N	13	N
(2368) Beltrovata	$2.28 \pm 0.2$	$15.5 \pm 5$	3.63	3.0	N	13	N
(3103) Eger	$1.16 \pm 0.16$	$58 \pm 7.5$	4.61	1.9	N	13	N
(3199) Nefertiti	$1.73 \pm 0.06$	$48 \pm 3$	4.19	2.0	N	13	N
(3288) Seleucus	$1.82 \pm 0.24$	$33 \pm 11$	3.67	3.0	N	13	N
(3362) Khufu	$0.67 \pm 0.07$	$24 \pm 4$	6.02	1.45	N	13	N
(3551) Verenia	$0.77 \pm 0.03$	$45 \pm 2$	3.58	3.1	N	13	N
(3554) Amun	$2.0 \pm 0.1$	$19 \pm 2$	6.11	1.25	N	18	N
(3757) 1982 XB	$0.54 \pm 0.03$	$22 \pm 2$	3.90	2.65	N	13	N

Table 9.1 – cont’d

Object	Diameter	Albedo	$T_J$	$q_{ap}$	Rotation?	Ref.	In Fig.
	(km)	(%)		(AU) <sup>a</sup>	<sup>b</sup>	<sup>c</sup>	9.4?
<i>NEAs with High <math>T_J</math> (cont’d)</i>							
(4688) 1980 WF	0.6±?	18±?	3.45	3.4	N	18 <sup>g</sup>	N
(6053) 1993 BW3	3.3 ± 0.6	18 ± 7	3.44	3.3	Y	24	N
(9856) 1991 EE	1.01 ± 0.15	30 ± 10	3.33	3.65	N <sup>i</sup>	23	N
1978 CA	1.86 ± 0.08	6.5 ± 0.6	5.44	1.4	N	15	Y

<sup>a</sup> Object’s aphelion distance.

<sup>b</sup> Has the object’s rotation been explicitly taken into account in the quoted values’

errors? Note that in some cases the integration times or the error bars themselves

may be so large as to obviate this point. Also, sometimes partial coverage of the rotational

variation was obtained.

*Table 9.1 – cont'd*

- 
- <sup>c</sup> References. 1 This Thesis. 2 Keller *et al.* 1986. 3 Jorda *et al.* 1999.  
4 Campins *et al.* 1995. 5 A'Hearn *et al.* 1989. 6 Campins *et al.* 1987.  
7 Cruikshank and Brown 1983. 8 Millis *et al.* 1988. 9 Lisse *et al.* 1999b.  
10 Campins *et al.* 1994. 11 Davies *et al.* 1993. 12 Jewitt and Kalas 1998.  
13 Veeder *et al.* 1989. 14 Lebofsky *et al.* 1978. 15 Lebofsky *et al.* 1979.  
16 Hudson and Ostro 1995. 17 Bell *et al.* 1988. 18 Tedesco and Gradie 1987.  
19 Mottola *et al.* 1997. 20 Tedesco 1992. 21 Veeder *et al.* 1984.  
22 Green *et al.* 1985. 23 Harris *et al.* 1998. 24 Pravec *et al.* 1997.  
25 Cruikshank and Jones 1977. 26 Morrison *et al.* 1976. 27 Lebofsky *et al.* 1981.  
28 Murchie *et al.* 1999. 29 Harmon *et al.* 1997. 30 Sar mecanic *et al.* 1997.  
31 Fernández *et al.* in preparation. 32 Sekanina 1988c. 33 Hanner *et al.* 1987.  
34 Campins and Schleicher 1995. 35 Fomenkova *et al.* 1995. 36 Hanner *et al.* 1996.
-

*Table 9.1 – cont’d*

---

<sup>d</sup> Reference only gives radius; no reliable optical cross section measurement yet exists to be able to calculate the albedo.

<sup>e</sup>  $T_J$  and  $q_{ap}$  are not really practical quantities for long-period comets.

<sup>f</sup> Reference only gives radius; albedo calculated using the known absolute magnitude.

<sup>g</sup> Unpublished, albedo mentioned in this reference without error bars; radius calculated using the known absolute magnitude.

<sup>h</sup> Explicitly mentions that these values are for the lightcurve maximum.

<sup>i</sup> Explicitly mentions that these values are for the lightcurve mid-brightness.

---

## 9.2 Comparing Radii and Albedos of “Cometary Nuclei”

We turn our attention to Fig. 9.1, a comparison of the albedos and diameters. The addition of several points to that graph with this thesis and by other workers in the last few years has started to fill out the “cometary” region on the graph. In the figure I have only used objects from Table 9.1 that have both a known diameter and an albedo, or at least claimed limits. There are two points that I want to make about the plot.

- Clearly there is some overlap between the NEAs and the cometary nuclei. The nuclei all have a geometric albedo  $p$  less than 14%, and several asteroids reside in this region as well, including some with high  $T_J$ . The overlap can be used to estimate the fraction of NEAs that are cometary nuclei. If we use  $p = 14\%$  as the boundary, seven of the forty asteroids are on the cometary side: 18%. Since not all of those seven need be dead comets, this could be interpreted as an upper limit. However there is an observational bias to discovering bright, shiny asteroids over dark ones, and hence thermal studies of NEAs will preferentially measure more of the high albedo objects, simply because we know more of them. This effect means that we may be underestimating the fraction of cometary NEAs – there are more (dark, carbonaceous) C- and D-type NEAs out there waiting to be discovered.

Of course, if one discovers asteroids through their thermal emission, the bias flows the other way, since then a lower albedo object would be easier to see (all else being equal). However currently the vast majority of NEAs are discovered optically.

Numerical integrations have been done showing that the NEA population’s source can be the Main Belt, via three main mechanisms (Greenberg and Nolan 1989, Migliorini *et al.* 1998): the 3:1 resonance with Jupiter, the  $\nu_6$  resonance with Saturn, and perturbations by Mars. However the existence of active comets in NEA orbits implies a non-negligible fraction of old cometary nuclei are there, and this ought to be taken into account when attempting to model the NEA taxonomic distribution. A more complete database of the taxonomic types of NEAs would in itself be valuable, if for example there are more C- and D-type NEAs (i.e., those with low albedo) than one would expect from the Main Belt delivery mechanisms, which predominately operate on the inner Main Belt where there are a higher fraction of S-type objects (Gradie *et al.* 1989). Recent estimates of the cometary contribution to the NEA population have been low, even approaching zero (e.g. Rabinowitz 1997), although others (e.g. Wetherill 1988) have suggested fractions higher than the 18% value I give above.

- There is no apparent constraint on the size of the nuclei; there are objects occupying every size scale from sub-kilometer to hundreds of kilometers. It is worthwhile to note that there are several more comets that are not listed in Table 9.1 that probably have sizes in the sub-kilometer range, and a few unlisted Kuiper Belt objects are probably larger than the plotted Centaurs. No thermal studies have been done of these objects, so the albedos are unknown; this is only based on optical studies and the range of possible albedos. For example, comet 45P/Honda-Mrkos-Pajdušakova has a diameter of less than 1 km even if the albedo is as low as 2% (Lamy *et al.* 1997). On the other extreme, Kuiper Belt object 1996 TO<sub>66</sub> is at least 450 km wide, using its absolute magnitude (Marsden 1997) and  $p \leq 14\%$ . The only

asteroids larger than this size are (1) Ceres, (2) Pallas, and (4) Vesta.

The KBOs and many of the objects in Fig. 9.1 have a common origin, and the question of the distribution of these original objects or their collisional fragments, will require many more hours at the telescope to build up a statistically significant sample. However it is gratifying that we have sampled almost three orders of magnitude of cometary sizes. There seems to be no doubt as to the existence of small comets, and interpreting that population in a size distribution of nuclei will likely shed light on the aging and active lifetime of these bodies.

### 9.3 Albedo and Orbital Parameters

A'Hearn *et al.* (1995), after analyzing the molecular abundances and dust production rates in the comae of about seven dozen comets, found a correlation between a comet's dust-to-gas mass ratio and its perihelion distance. They concluded that this was due to the effect of the solar heating cycle on the mantle of the nucleus – the mantle is presumably thicker for smaller perihelia, making it harder for grains to be entrained in the escaping gas, leading to a lower dust-to-gas ratio. In Fig. 9.2 I have plotted the cometary albedos versus perihelion distance, but there does not yet seem to be any clear trend. Thus, while there is some thermal processing of the surface layers of a comet, this does not appear to influence the albedo. This may argue against the existence of near-surface ice on cometary nuclei, since in that case one might expect the objects with larger perihelia – e.g., the Centaurs – to be more reflective. This would corroborate the findings from simultaneous IR and optical observations of nuclei that indicate cross section, and not emissivity or albedo, cause the brightness variations (e.g., A'Hearn *et al.* 1989). The cometary ice appears to be in a matrix with the rock in a porous subsurface layer. However adding several more objects to Fig 9.2 would strengthen (or refute) this conclusion.

Figure 9.3 compares the albedo and the Tisserand invariant. The dashed line marks the nominal traditional separation between asteroids and comets. There is no apparent trend with this parameter either, reiterating that the albedos are seemingly not tied to the orbital characteristics of the objects, at least with the sample we currently have. Had the aging of a comet affected the albedo, one might have expected that a comparison of Halley Family with long-period comets and Centaurs with short-period comets would have shown different clustering. No such trend is evident with the current sample.

### 9.4 A Motivator for the Future

In Fig. 9.4 I have shown a current estimate of the size distribution of cometary nuclei. In this case I have defined cometary nuclei very liberally, including many of the asteroids that I mentioned in the previous subsection. The 25 objects that were used to make this graph are noted in Table 9.1; note that I have not included the three Centaurs. Also plotted are three possible size distribution power laws.

The value of the power law exponent in a system of colliding particles that have some self-gravity has been the target of various numerical models over the years. Davis *et al.* (1985) find that the cumulative power law goes as  $D^{-2.5}$  for objects smaller than 20 km wide and flattens out for larger objects. A cometary distribution

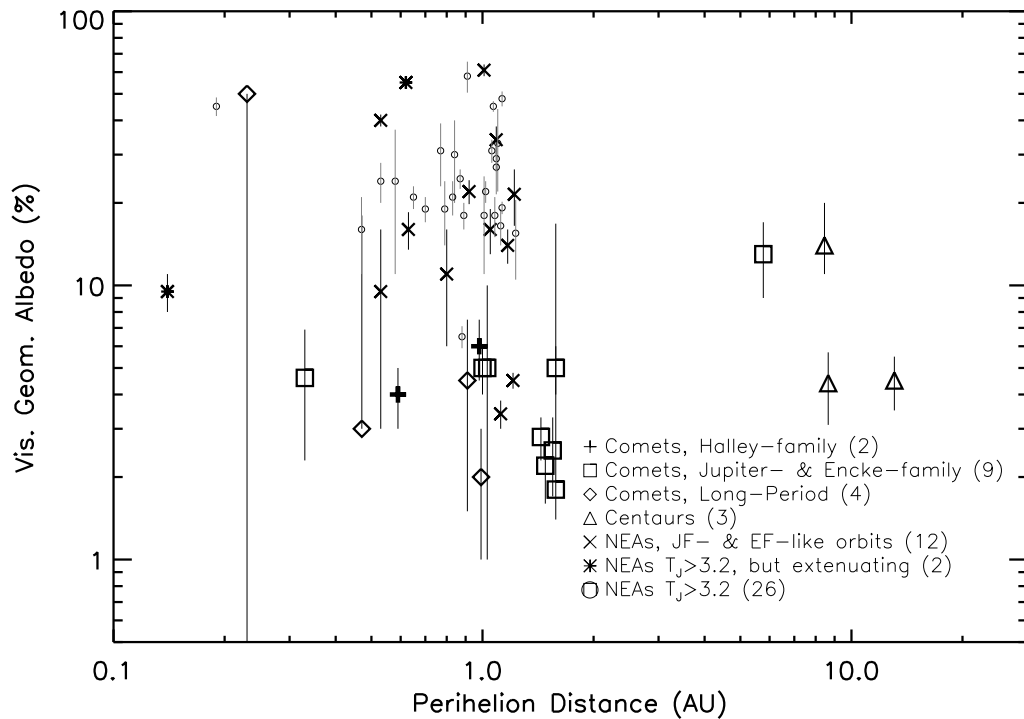


Figure 9.2: A comparison of the albedos of cometary nuclei and related objects to their perihelion distance. No trend is apparent, although A'Hearn *et al.* (1995) find that the Sun thermally processes the mantle and affects the size distribution of the dust entrained with the gas. This affect does not seem to manifest itself in albedo, however.



that approaches this would indicate a high frequency of collisions among the comets; conversely, a different size distribution shape would contradict this idea. Clearly the current distribution is nowhere near this power law, being more proportional to  $D^{-1}$ , but the sampling is of course not complete and it remains to be seen how this law will change in the coming years as more thermal studies are done of comets and NEAs.

Connected to this issue are the separate size distributions of the Oort Cloud comets – today’s Halley Family and long period objects – and the Kuiper Belt comets – today’s current KB residents and the Jupiter Family objects. The collision histories of the two sets of objects differ (Stern 1988, Stern 1995), and presumably once a large number of cometary nuclei are sampled the evidence will be there.

In an ideal situation, we could sample many long-period comets that are new in the Oort sense and see what the current distribution of sizes is *today* in the Oort Cloud. Information on the rotational state of these bodies would also determine just how pristine the objects are – are they rotating faster or slower than the current inner Solar System population? Since splittings and non-gravitational forces act on the active comets and affect the rotation rate, in addition to any repercussions of the comet’s most recent collision, it would be interesting to see what the relatively pristine OC comets were originally like. One ought to note that there are precisely zero Oort-sense new long-period comets listed in Table 9.1. This is mainly because there are simply fewer “new” Oort Cloud comets discovered compared to “old” ones.

The cometary connection with the asteroids needs to be solidified with more observational data. There seems to have been a deceleration in the number of thermal studies of NEAs in the past decade; one hopes that this trend will be reversed since there are about 800 NEAs currently known, with new discoveries being made at an increasing rate due to the fecundity of asteroid search programs. Even optical information, to obtain a complete census of the representation of the taxonomic classes among the NEAs, would be useful, since that can be correlated with the taxonomic gradient in the other source region, the Main Belt.

Another, more direct approach is to look for faint gas emission around near-Earth asteroids. Comet Wilson-Harrington is the most successful example of this phenomenon: the comet was discovered in 1949, then re-discovered in its asteroidal incarnation in 1979, and the two apparitions were linked in 1992 (Bowell and Skiff, reported by Marsden 1992). I discussed the cometary nature of the 1949 data in a separate work (Fernández *et al.* 1997). A deep search for any OH signature around several NEAs would provide strong, direct (and modern) evidence for the evolutionary connection between the asteroids and comets.

## 9.5 Future Data Rates

The future of thermal observations of comets is bright. *SIRTF* will be available in a few years to give us unprecedented sensitivity in the thermal regime. In principle, since the lifetime of the satellite is expected to be three to five years, a systematic survey of all of the Jupiter Family comets could be done. Furthermore, the size distribution of the Kuiper Belt objects could be measured, since the sensitivity will finally allow us to measure the trickle of blackbody radiation coming from those objects. This is all contingent on the allocation of sufficient observing time.

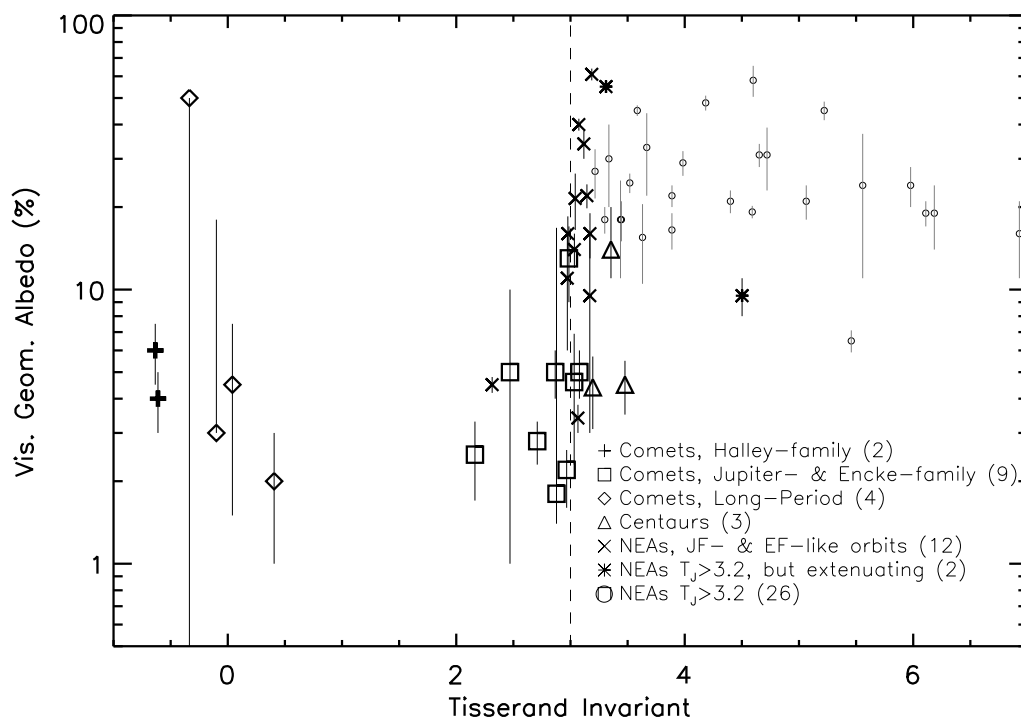


Figure 9.3: The Tisserand invariant is compared to the albedos. An aging affect might have manifested itself in albedo differences between long-period and Halley family comets, and Jupiter family and Centaurs, but no such trend is yet in evidence.

It should be clear from this thesis that the advent of large arrays of 10 and 20  $\mu\text{m}$  detectors was critical for the success of this work, and that the continued increase in size and sensitivity will make it easier to sample more comets from the ground in the coming years. Based on our experience, one detailed study of a short-period comet and quick looks at two other comets (short- or long-period) can be done per mid-IR observing run. An obvious benefit of having frequent observing runs for scheduled short-period comets is the increased probability of being at a telescope when a newly discovered long-period comet (unknown at the time of the telescope's proposal deadline) is available. There are approximately 3 short-period comets worthy of intense study per year, and if a few fortuitous comets are also observable, then optimistically, we could have some physical information about a dozen cometary nuclei every two to three years or so. The observing efficiency is even better for NEAs, since there are more of them. By the time the *Rosetta* spacecraft encounters comet 46P/Wirtanen in 2012, we may start to have a handle on the ensemble properties of the nuclei.

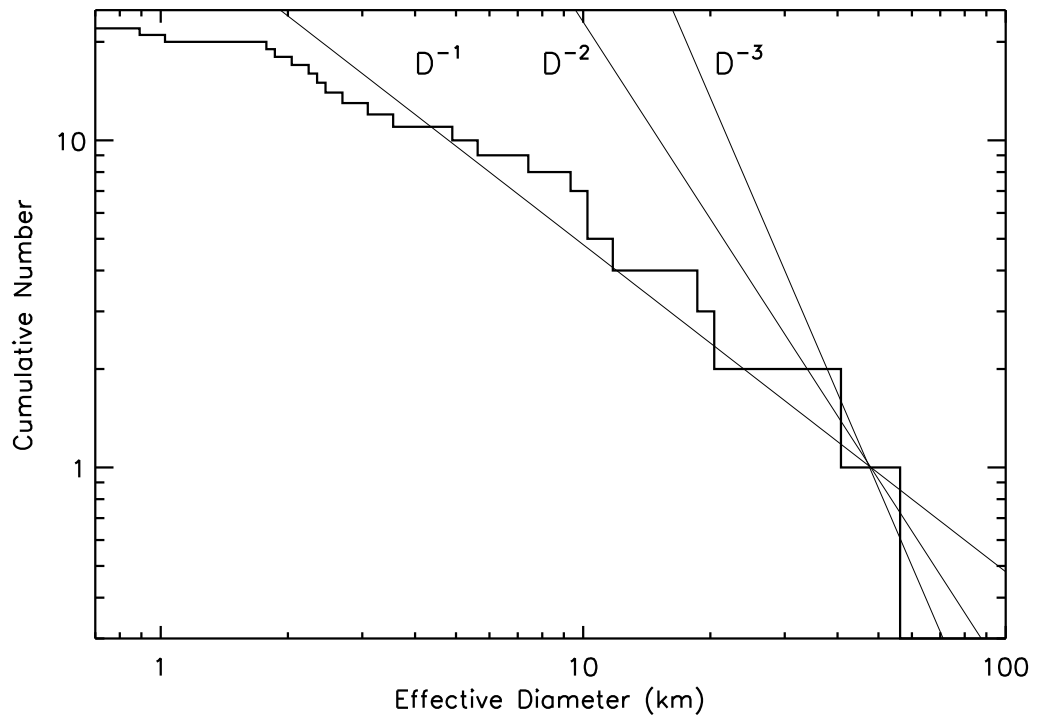


Figure 9.4.: The current size distribution of cometary nuclei and related objects that may be nuclei. This is not to claim that the sample of objects is complete on any size scale. The eventual slope of the real distribution function will give clues to the collisional history of the cometary population.

